

Subband resonance of electrons on Si(110)

Soe-Mie Nee,* U. Claessen, and F. Koch

Physik-Department, Technische Universität München, D-8046 Garching, Federal Republic of Germany

(Received 10 May 1983; revised manuscript received 7 September 1983)

Infrared resonant absorption from electron subbands on n -type Si(110) is studied for surface densities N_s up to $1.2 \times 10^{13} \text{ cm}^{-2}$. The $0 \rightarrow 1$ transition is observed in the *perpendicular* and, provided that the polarization is along the [110] axis in the surface, in the *parallel*-excitation modes. A distinct splitting on the order of 30% in N_s is found for the two modes. It results from the absence of the depolarization shift (i.e., $\alpha=0$) in parallel excitation. The comparison with a calculated subband splitting permits the determination of the exciton energy. The resonance shifts rapidly to higher energy with rising temperature in the range 4.2–200 K.

I. INTRODUCTION

Infrared absorption spectroscopy has served to characterize the electronic subband states of an interfacial charge layer. Not only have subband energies been measured by this means, but a number of specific features of the dynamics of the resonant excitation have attracted attention. A survey of such work is contained in Ref. 1.

The most thoroughly studied model system of the electric subbands has been the Si(100) n channel. The lowest-lying electron surface bands are formed from electronic states of the pair of constant-energy ellipsoids whose major axis is aligned with the surface normal. The $n=0$ ground-state subband and higher $n=1, 2, 3$, etc., levels are twofold valley degenerate ($g_v=2$). Subband resonance in this system of levels can be excited only by ir radiation polarized perpendicular to the sample plane. This polarization is achieved either in the strip-transmission-line geometry of Ref. 2 or the prism-coupling technique as in Refs. 3 and 4. The dominant absorption line is the $0 \rightarrow 1$ transition from the $n=0$ ground state to the $n=1$ subband.

The ir-excited $0 \rightarrow 1$ resonance is linked with an excitation energy \tilde{E}_{01} . The latter is derived from the subband-energy separation $E_{01} \equiv E_1 - E_0$ by adding two distinct physical corrections involving the nature of the excitation process itself. The first of these is variously referred to as resonant screening, local-field correction, or depolarization shift. Its role in subband resonance was first recognized in Refs. 5 and 6. It represents the influence of the dipole field of all the other coherently vibrating surface charges on the particular electron under consideration. The effect of depolarization is to shift the observed maximal absorption from E_{01} to higher energy where the dielectric response function of the single particle has a zero. In Ando's description⁷ the depolarization shift is expressed by a dimensionless α , such that $\tilde{E}_{01} = E_{01} \sqrt{1 + \alpha}$. The shift is 20–30% in typical subband-resonance experiments. It has been measured in experimental work on InSb, InAs, GaAs, and $\text{Hg}_{1-x}\text{Cd}_x\text{Te}$.

The second correction, which features prominently in the Si subband resonance, is a final-state interaction effect, termed the excitonlike shift by Ando.⁷ It represents the

energy of the Coulomb interaction between the electron excited to $n=1$ and the hole left behind in the charge distribution of the $n=0$ ground state. For Si, with its relatively high m^* and not-so-high ϵ , this correction is important and makes a sizable contribution to \tilde{E}_{01} . Its sign is opposite to the depolarization effect. Its magnitude β as calculated by Ando is close to the value of the depolarization. The net resonance energy for Si is expressed as $\tilde{E}_{01} = E_{01} \sqrt{1 + \alpha - \beta}$. The net correction as calculated by Ando⁷ is quite small ($\sim 5\%$) for typical charge layers on Si(100) and depends on the density N_s . Confirmation that this description is reasonable comes from the involved analysis of tilted-magnetic-field data.^{8,9} There exists no direct measurement of either α or β , and a critical comparison with theoretical literature reveals differences in the β value obtained with density-functional methods or diagrammatic summation.¹⁰

It has been recognized^{11–14} for some time that electron subbands on Si(110), because of the tilted-ellipsoid geometry, can be excited both in the perpendicular subband geometry and with parallel-polarized radiation. Some preliminary results on (110) subband spectroscopy exist in the literature^{13,14} and are circulated as private communication.¹² The experimental uncertainties in the existing (110) data make an exacting comparison with theory difficult. Moreover, the work in Refs. 13 and 14 could not distinguish between the perpendicular- (\perp -) and parallel- (\parallel -) excited resonances.

In view of what is known about the two modes of excitation in other materials¹⁵ and the potential of such measurements in sorting out the α and β contributions for Si, it appeared to us a challenge to examine the polarization effects for (110) subbands. A recent theoretical paper,¹⁶ with explicit numerical results for Si(111), shows that a large splitting of \parallel - and \perp -excited resonances occurs because of the depolarization α . The final-state interaction effect represented by β is the same in the two modes, so that the comparison \parallel vs \perp measures α . The experimental result in Ref. 17 fails to show the expected splitting.

This paper describes an investigation of subband resonance on Si(110). After some discussion of the principle of parallel excitation on Si(110) in Sec. II, we turn in Sec. III to the experimental results. The final Sec. IV summarizes the conclusions.

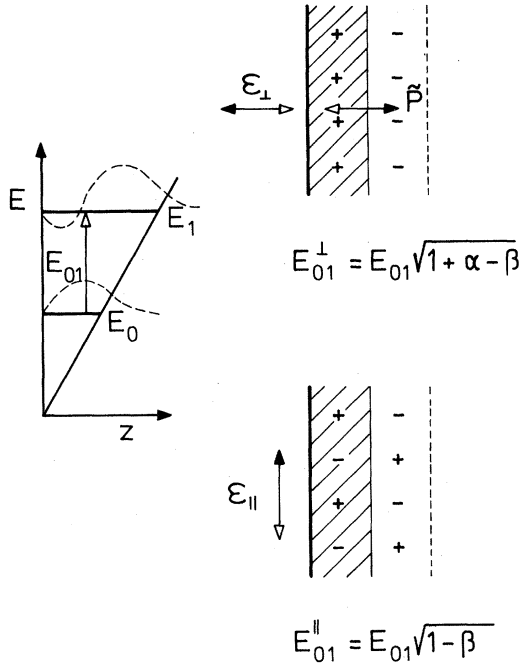


FIG. 1. Subband energies E_0, E_1 and the excitation modes E_{01}^\perp and E_{01}^\parallel assuming a symmetry-related cancellation of the depolarization in E_{01}^\parallel .

II. SUBBANDS ON Si(110) AND THE PARALLEL-EXCITATION MECHANISM

Because subbands are eigenstates of the \hat{z} -directed motion in the surface potential well $V(z)$, conventional resonance experiments involve radiation polarized perpendicular to the semiconductor surface. The mode excited coherently by the electric field ϵ_\perp in Fig. 1 is what we will refer to as the E_{01}^\perp resonance. It is Ando's \tilde{E}_{01} as discussed in the Introduction and is fully affected by the α and β shifts.

With the work on InSb (Refs. 15 and 18) it was first recognized that a parallel-excited resonance E_{01}^\parallel is also possible. The coupling mechanism in this case is provided by the nonparabolicity of the subbands. In a particularly lucid derivation it has been shown by Zawadzki¹⁹ that parallel excitation is a higher-order process that results from band mixing by the surface electric field. As such, the parallel resonance is usually an order of magnitude smaller than the resonance in the perpendicular conductivity.²⁰ The energy splitting between the E_{01}^\perp and E_{01}^\parallel resonances, perpendicular as observed in experiments on InSb, InAs, and $\text{Hg}_{1-x}\text{Cd}_x\text{Te}$,²¹ is ascribed to the fact that $\alpha=0$ in the parallel mode. Because, in addition, the excitonlike shift β is estimated to be negligibly small in these materials, the E_{01}^\parallel resonance has been equated with the subband splitting E_{01} .

It is instructive to examine why $\alpha=0$ for the \parallel excitation of the nonparabolics. The reason is that the matrix element coupling the parallel electric field to the subbands

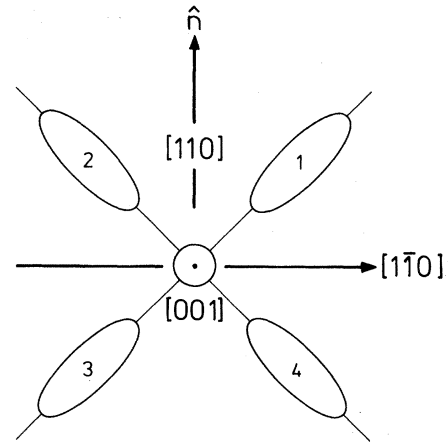


FIG. 2. Electron constant-energy ellipsoids for the Si(110) plane.

involves the momentum k_\parallel linearly. Thus, electron states on opposite sides of the symmetric Fermi distribution contribute with opposite phases to the \hat{z} -directed current. For such anticorrelated motion of electron pairs with $\pm k_\parallel$ there is no net current normal to the surface. The perpendicular polarization vanishes and there is no α shift. This is the situation sketched in the lower part of Fig. 1.

The $\alpha=0$ mode observed in the resonant Raman scattering experiments²² using crossed polarization of the incident and scattered light involves yet a different mechanism. The scattering in the spin-flip mode is attributed to a spin-density fluctuation. The strong coupling of the light to this mode is made possible by the spin-orbit effects in the valence band of GaAs. The spin-density mode has no electric dipole moment and consequently the excitation energy does not involve the polarization shift.

The E_{01}^\parallel excitation of the Si(110) electron subbands is possible for a very different reason, one that does not involve the fine points of higher-order processes. The ground-state, $n=0$ subband is formed from the four tilted ellipsoids (labeled 1–4) in Fig. 2. Higher states of this $g_v=4$ system are subbands $n=1, 2$, etc. The two in-plane, constant-energy ellipsoids form the subbands $n=0', 1', 2'$, etc. They are not occupied at low temperatures and the usual densities N_s of the surface layer. The resonance of the unprimed subband states can be excited in both \perp and \parallel modes, because the kinetic energy operator of each tilted ellipsoid has the form

$$\mathcal{H}_1 = \frac{1}{4} \vec{p}^T \begin{pmatrix} 2m_t^{-1} & 0 & 0 \\ 0 & (m_t^{-1} + m_l^{-1}) & \pm(m_t^{-1} - m_l^{-1}) \\ 0 & \pm(m_t^{-1} - m_l^{-1}) & (m_t^{-1} + m_l^{-1}) \end{pmatrix} \vec{p}$$

when the in-plane directions \hat{x} and \hat{y} are along the [001] and [1 $\bar{1}$ 0] directions, respectively, and the normal [110] coincides with \hat{z} . The m_l and m_t are the usual longitudinal and transverse effective-mass values. The \pm signs depend on the particular ellipsoid in question.

As discussed in Refs. 11 and 16, the existence of the

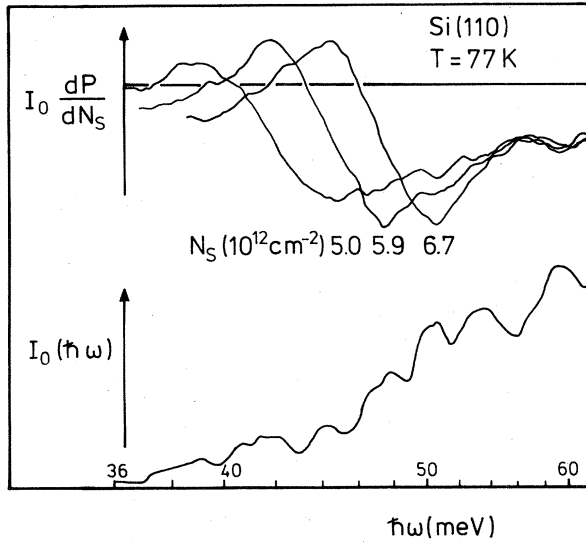


FIG. 3. Transmission-derivative data obtained with a grating spectrometer for various densities N_s . $I_0(\hbar\omega)$ is the intensity function.

off-diagonal components causes coupling of an rf electric field along \hat{y} to the \hat{z} -directed subband motion. For the fully degenerate, $g_v=4$ ground state, the net \hat{z} -directed current in a parallel field vanishes because of the anticorrelated motion of carriers in the symmetry-related ellipsoids. It follows that for the E_{01}^{\parallel} mode in the $g_v=4$ state, the depolarization α vanishes.

Measurements of the Shubnikov–de Haas (SdH) oscillations have in the past been interpreted as if $g_v=2$. A great deal of discussion of this surprising result can be found in the literature.¹ It has been ascribed to complex many-body effects on the one hand and to the dynamics of filling Landau levels in slightly strain-shifted valleys on the other. The work in Ref. 11, in particular, has considered the effect on the subband resonance if g_v were equal to 2, with electrons occupying either ellipsoids 1 and 3 or 2 and 4 only. It has been shown that the $g_v=2$ parallel-excited resonance would then be depolarization-shifted to a higher energy. That α would not equal zero for the E_{01}^{\parallel} excitation in this case is easy to see from the symmetry of the ellipsoids. If only 1 and 3 are occupied, then a net \hat{z} -directed current results when the field ϵ is along \hat{y} . It is equally easy to convince oneself that this current, although finite, is less than its value for ϵ along \hat{z} . It appears that as a consequence the depolarization shift for E_{01}^{\parallel} in the $g_v=2$ case is somewhat less than that for the E_{01}^{\perp} resonance. Only if the ellipsoid were strongly elongated, with $m_l/m_t \gg 1$, do we agree with the statement made in Ref. 11 to the effect that “the absorption spectrum for the transmission line configuration (E_{01}^{\perp}) is essentially the same as that in the simple transmission configuration (E_{01}^{\parallel}).”

It is clear that subband resonance, in particular a careful comparison of E_{01}^{\perp} and E_{01}^{\parallel} on Si(110), can, in conjunction with a calculation, resolve the “ $g_v=2$ or 4” controversy. The fact that Refs. 14 and 17 could not really dis-

tinguish between E_{01}^{\perp} and E_{01}^{\parallel} , where theory predicts a rather sizable difference^{11,16} provided a major incentive for this work.

III. EXPERIMENTAL RESULTS

A. Samples and measuring techniques

All samples were prepared from a single 2-in., n -type ($\sim 2 \times 10^{15} \text{ cm}^{-3}$) wafer oxidized to a thickness of $2600 \pm 20 \text{ \AA}$. The wafer was annealed according to standard procedures in order to reduce the interface charge and states to acceptable levels.

Specimens are cut to $6 \times 8 \text{ mm}^2$ and provided with an active gate $4 \times 6 \text{ mm}^2$. For \parallel excitation the gate is a transparent NiCr layer. Thick Al ($> 5000 \text{ \AA}$) gates are used with samples in the strip-transmission line. To achieve good relative accuracy in a comparison of \parallel and \perp data, the same sample is recoated with Al after completion of the parallel-excitation experiments. Typical flat-band voltages in the 4.2-K capacitance-voltage relation are in the (-1 to -3)-V range.

Measurements of the ir absorption are made with the grating spectrometer used in earlier work on InSb and InAs (Refs. 15 and 18) and with the conventional far-infrared (fir) laser spectrometer. The latter is employed with the sample mounted in the strip-transmission line for \perp excitation. For measurements in the parallel mode with either the grating spectrometer or the laser, we use transmission at normal incidence. The grating spectrometer has provided parallel-excitation data for $\hbar\omega \geq 36 \text{ meV}$.

The grating system provides the option to make an $\hbar\omega$ sweep of the excitation energy, or as usual in subband spectroscopy, to vary the surface density N_s at fixed $\hbar\omega$. The quality of frequency-sweep data can be judged from the experimental curves in Fig. 3. The curves each need to be normalized and corrected by the intensity function, which contains a number of distinct structures. The normalized signal is the absorption derivative dP/dN_s vs $\hbar\omega$. The resonance represents the $0 \rightarrow 1$ transition of the electrons. For energies $\hbar\omega \geq 36 \text{ meV}$ such data compare favorably with frequency-domain data using a Fourier-transform spectrometer.^{13,14,17}

In all the parallel-mode measurements the polarization vector can be adjusted at any angle to the crystal axes in the sample plane by using a linear polarizing filter mounted above the sample. The temperature can be varied from 4.2 to 300 K.

B. Parallel-excitation spectra

For Si(110) electrons one expects an allowed, parallel-excited resonance. The previous Fig. 3 is obtained in that mode. As is usually the case for accumulation, only the $0 \rightarrow 1$ resonance can be clearly identified.

Figure 4 shows N_s -sweep spectra for parallel polarization at 77 K and $\hbar\omega = 17.6, 30.2, \text{ and } 41.3 \text{ meV}$. In particular, at low $\hbar\omega$ (17.6 meV) the resonance contribution is difficult to separate from structure in the background absorption which includes a peak at low N_s . Clarity is achieved by making use of the additional degree of freedom of the polarization. When the currents are rotated to

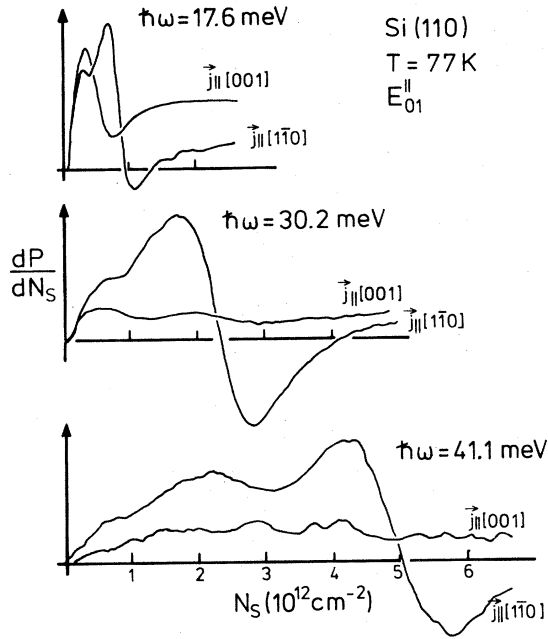


FIG. 4. Current rotation curves in the (110) plane. The resonance appears only with $j_{||}([1\bar{1}0])$ at all densities.

the [001] axis in the sample plane, the $0 \rightarrow 1$ resonance signal is caused to disappear, leaving the background signal. The low- N_s peak that appears so prominently in the 17.6-meV curve is typical of a sample contaminated with interface charge.²³ It is linked with dynamic conductivity of electrons moving in the perturbing potential of the interface ions.²⁴ The impurity-peak amplitude is large in the range 10–20 meV, and the signal can be seen both with $[1\bar{1}0]$ and [001] polarization. The subband resonance, as the rotation experiment unambiguously demonstrates, comes from ellipsoids tilted out of the surface in the (001) plane. The polarization experiment in itself, however, cannot distinguish between the degeneracies $g_v = 2$ or 4.

C. Parallel versus perpendicular excitation

The ease with which parallel-mode data can be obtained on Si(110) (Figs. 3 and 4) makes possible an exacting comparison with the conventional, perpendicular excitation of the laser spectrometer at fixed $\hbar\omega$. Figure 5 shows a comparison of the two modes at $\hbar\omega = 17.6$ and 30.2 meV both at 77 K and for the same sample. In view of what had been said in the literature¹⁴ we were surprised to find such a distinct, easily measured splitting between the two modes. The resonance position at the higher of the two frequencies is practically doubled in parallel excitation. The N_s values are high enough so that the absolute errors in flat-band determination are small. Moreover, the comparison makes use of the same sample and leaves no uncertainty that there is a difference in the two modes of excitation. In view of the discussion in the preceding sections, the data are evidence for a sizable depolarization shift α in the perpendicular mode and its absence in the parallel-excited resonance. The data argue for $g_v = 4$, at

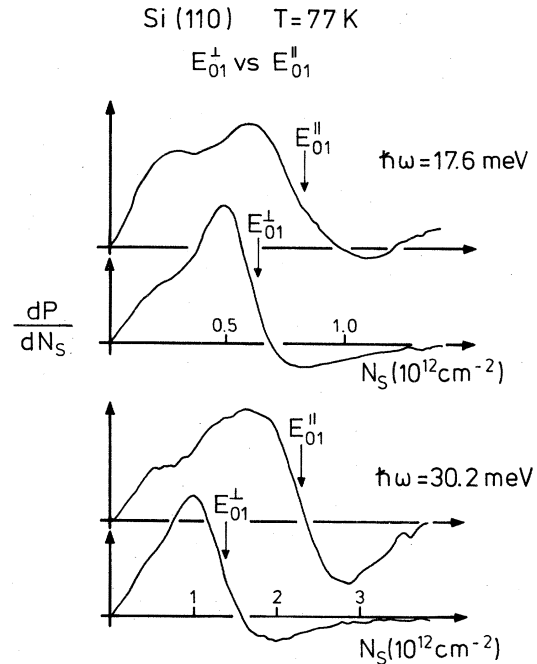


FIG. 5. Parallel- and perpendicular-excited subband resonances on Si(110) at 77 K.

least at the temperature (77 K) of the experiments.

The possibility that the temperature would act to destroy the $g_v = 2$ ground state prompted us to repeat the experiments at 4.2 K. It is at liquid-He temperature that the SdH experiments, which originally led to the $g_v = 2$ hypothesis, are made. Figure 6 shows the low-temperature

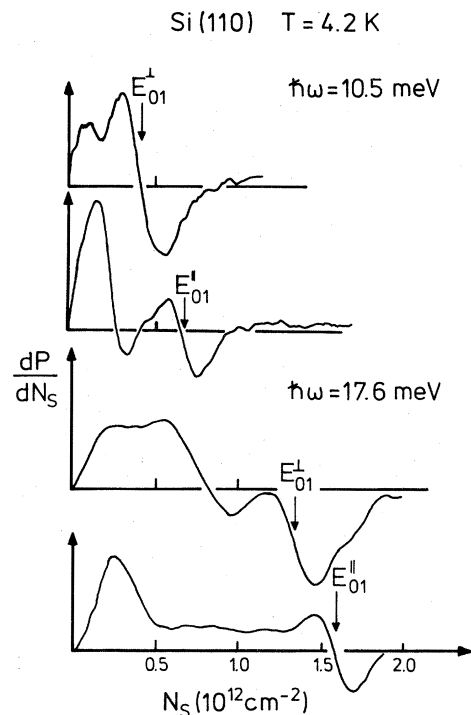


FIG. 6. Parallel- and perpendicular-excited subband resonances on Si(110) at 4.2 K.

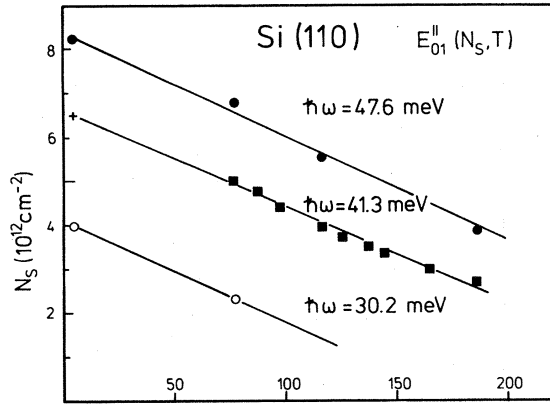


FIG. 7. Temperature dependence of the E_{01}^{\parallel} -resonance position at different $\hbar\omega$.

result for the comparison of \parallel - and \perp -excitation modes. All the lines have shifted by a substantial amount in N_s . The splitting between the two modes remains. We must conclude that the α shift remains to distinguish E_{01}^{\parallel} and E_{01}^{\perp} at low T .

The E_{01}^{\perp} and E_{01}^{\parallel} resonances are preceded at low N_s by additional absorption structures already mentioned in connection with Figs. 4 and 5. The current rotation experiment (Fig. 4) has demonstrated that for the \parallel mode most of the precursor structure is not a subband signal from the tilted ellipsoids. We find that the precursor varies from sample to sample and can be influenced by the drift of ions to the interface. It is quite different for the two modes of excitation. The origin of the structures is under further investigation.²⁴

D. Temperature dependence

Comparison of Figs. 5 and 6 shows the effect of temperature on the N_s position of the resonances. Such dependence arises from a number of distinct physical effects. The primary cause of shifts to lower N_s at fixed $\hbar\omega$ is the thermal occupancy of higher-lying subband levels. By occupying states with larger penetration depth the charge is spread out. The screening nearest the surface, where the $n=0$ electrons are bound, is reduced, and the binding energy E_0 is increased. Thus, the separation E_{01} becomes greater. In addition, the many-body energies contributing in the form of the exchange-correlation potential, the excitonlike shift β and the depolarization effect α , are changed with T .²⁵

Both the large magnitude of the position shift and its sign suggest that for (110) electrons the dominant temperature effect is the occupancy of the $0'$ level formed by the two in-plane ellipsoids, and that may be expected to lie just above E_F . The relevant quantity for repopulation effects is the energy $E_{0'} - E_F$ compared to kT . In the accompanying Fig. 7 we have plotted the parallel-mode-resonance position versus T at one particular energy. A few points for other frequencies are also entered for comparison. It is not at all evident why the relation of N_s and T should be a straight line in Fig. 7, nor for that matter

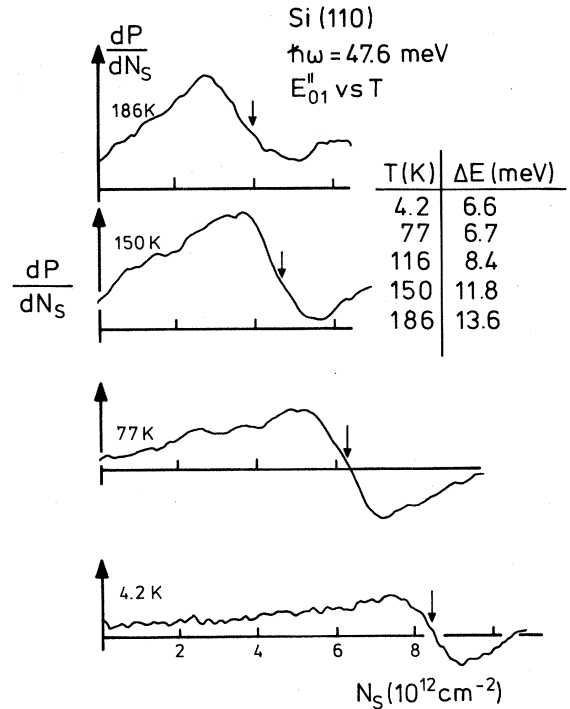


FIG. 8. The E_{01}^{\parallel} resonance and its linewidth ΔE at different temperatures.

why the slopes are so similar.

As in previous work on Si(100) (Ref. 26) the resonance broadens with rising T gradually. The relative change in linewidth is usually less than the corresponding change in the surface mobility. Because our sample lacks source-drain contacts, the latter has not been measured simultaneously, but the analogy with Si(100) data is evident. The sequence of curves in Fig. 8 covers the temperature range 4–186 K. The inset gives the linewidth in meV, obtained by measuring the peak-to-peak separation ΔN_s and multiplying by the slope of the energy-versus- N_s curve.

E. Resonance energies E_{01}^{\perp} and E_{01}^{\parallel} vs N_s

The objective of a subband spectroscopy experiment is the determination of excitation energy over the complete range of N_s . The strong T dependence of the data and the difficult interpretation of this effect makes it essential to use 4.2-K data in a comparison with theory. The curves in Fig. 9 are the averaged wisdom of many measurements. The lines are marked E_{01}^{\perp} and E_{01}^{\parallel} for the perpendicular- and parallel-excited resonances. Data points for 4.2 K only have been entered in Fig. 9. The range of N_s is limited by the breakdown strength of the SiO_2 to about $1.3 \times 10^{13} \text{ cm}^{-2}$ on our large-area samples.

There exist a number of calculations of the subband energy with which the data in Fig. 9 can be compared. Up to $1.5 \times 10^{12} \text{ cm}^{-2}$ Ando⁷ gives both the subband splitting E_{01} and the excitation energy E_{01}^{\perp} . Because of the near coincidence of α and β in Ando's⁷ calculation, E_{01} and E_{01}^{\perp} could not really be distinguished on the scale of Fig. 9. In the range up to $N_s = 1.5 \times 10^{12} \text{ cm}^{-2}$, Ando's E_{01}

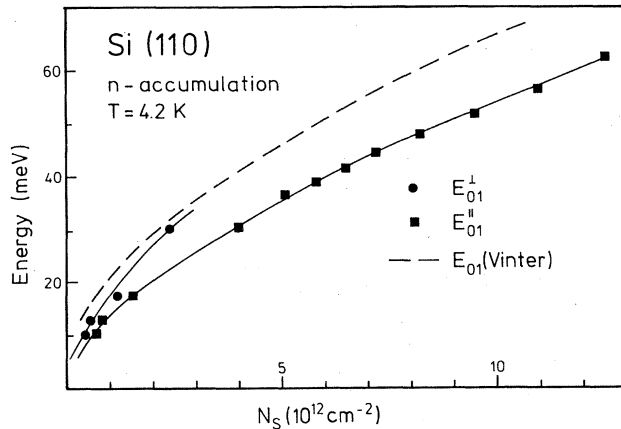


FIG. 9. Experimental values for E_{01}^{\perp} (●) and E_{01}^{\parallel} (■) vs N_s . The dashed line is the subband splitting E_{01} after Vinter (Ref. 27). The estimated uncertainty is of the order of the size of the experimental points.

coincides with a calculation due to Vinter.²⁷ The experimental E_{01}^{\perp} points are close to, but consistently below, the calculated E_{01} . The E_{01}^{\parallel} values are distinctly shifted to higher N_s , so much, in fact, that we are at a loss to understand why Refs. 13 and 14 failed to resolve the splitting. The experimental points of Ref. 14 ($0.5 \leq N_s \leq 1.5 \times 10^{12} \text{ cm}^{-2}$) lie just slightly above the broken line.

While the splitting of E_{01}^{\perp} and E_{01}^{\parallel} in Fig. 9 provides an experimental measure of α , the comparison of E_{01}^{\parallel} with the calculated E_{01} yields the value of the excitonlike shift β . There exists no explicit calculation of either α or β over the N_s range covered by the experiments, so that a more detailed comparison is not warranted. By comparison with the (111)-plane numerics in Ref. 16 we note that the E_{01}^{\perp} and E_{01}^{\parallel} splittings are reasonable.

IV. CONCLUDING REMARKS

The primary result of this work has been to establish that for Si(110) there are two distinctly different modes of excitation. Parallel- and perpendicular-excited subband resonances are split in energy by a substantial amount.

The observations are as expected for a sample with $g_v = 4$. We have made magnetoconductivity measurements using microwaves on our capacitor-type samples. SdH oscillations show up weakly above ~ 8 T. The SdH period is consistent with $g_v = 2$, but the limited field range (8–10 T) did not permit an unambiguous assignment of the valley degeneracy. The (110) samples in Refs. 13 and 14 are also for the $g_v = 2$ type for the analysis of SdH oscillations.

Because the depletion charge is not specified for the (110) data in Refs. 13 and 14, it is not possible to compare directly with the energy values $E_{01}(N_s)$. The points lie consistently above the dashed line E_{01} in Fig. 9. This

would be expected for \perp excitation and a depletion charge of order 10^{11} cm^{-2} .

The present data obviates the need for depletion-charge determination by using n accumulation. By extending the measurements to high N_s , where the possible errors in flat-band determination are negligible, we provide data that can be critically compared with calculations. The parallel-mode data (E_{01}^{\parallel}) are clearly not equal to the calculated E_{01} , and thus points to a sizable exciton shift.

The comparison with theory is by no means a simple exercise. There are a number of points which need to be considered quite carefully in each of the possible comparisons. The simplified discussion in terms of the α and β has leaned on the two-level model, which ignores the influence of the polarizability associated with transitions $0 \rightarrow 2$, $1 \rightarrow 2$, etc., on the position of the E_{01}^{\perp} resonance. A calculation such as in Ref. 16 is required to correctly interpret the difference E_{01}^{\perp} and E_{01}^{\parallel} . An α calculated within the approximations of the two-level system is only a rough check. Implicit in this comparison is the assumption that the exciton shift β is independent of the mode of excitation. Within the framework of approximations in Ref. 16 this appears to be the case, but it has not been demonstrated rigorously.

Because of these caveats we have preferred in Fig. 9 to stress the comparison between the E_{01}^{\parallel} data and the subband-energy calculation for E_{01} . To the extent that the E_{01}^{\parallel} does not involve α at all and that the straightforward energy calculation is thought to be reliable, this comparison identifies the exciton effect to good accuracy. In this sense we hope that the $E_{01}^{\parallel}(N_s)$ data in Fig. 9 provides a proving ground for the many-body-effect calculations of the surface charge layer on Si.

A brief mention of amplitudes is necessary. The experimental amplitudes are difficult to determine reliably in modulation experiments and for the interference-prone parallel-layer sample geometry. All the experimental curves are given in arbitrary units. A typical magnitude of the integrated resonance signal for $N_s = 5 \times 10^{12} \text{ cm}^{-2}$ in parallel excitation is 0.5% of the transmitted intensity. The signal appears smaller than expected for an allowed transition at such an N_s . We have found that subband resonance on Si(100) is reduced by a large factor when interface charge is introduced²⁴ and believe that the situation is similar for the (110) plane. Thus, the appearance of the precursor structure and a loss of subband-oscillator strength are linked on (110) samples. It is instructive to compare with Fig. 9 in Ref. 28.

ACKNOWLEDGMENTS

We thank C. Mazuré and F. Martelli of our laboratory for providing much of the 4.2-K data necessary for the completion of this work. This work was supported financially by the Deutsche Forschungsgemeinschaft (Sonderforschungsbereich 128).

- *Permanent address: U.S. Naval Weapons Center, China Lake, CA 93555.
- ¹T. Ando, A. B. Fowler, and F. Stern, *Rev. Mod. Phys.* **54**, 437 (1982).
- ²A. Kamgar, P. Kneschaurek, G. Dorda, and F. Koch, *Phys. Rev. Lett.* **32**, 1251 (1974).
- ³B. D. McCombe, R. T. Holm, and D. E. Schafer, *Solid State Commun.* **32**, 603 (1979).
- ⁴J. Scholz and F. Koch, *Solid State Commun.* **34**, 249 (1980).
- ⁵W. P. Chen, Y. J. Chen, and E. Burstein, *Surf. Sci.* **58**, 263 (1976).
- ⁶S. J. Allen, D. C. Tsui, and B. Vinter, *Solid State Commun.* **20**, 425 (1976).
- ⁷T. Ando, *Z. Phys. B* **26**, 263 (1977).
- ⁸W. Beinvogl and F. Koch, *Phys. Rev. Lett.* **40**, 1736 (1978).
- ⁹T. Ando, *Phys. Rev. B* **19**, 2106 (1979).
- ¹⁰B. Vinter, *Phys. Rev. B* **15**, 3947 (1977).
- ¹¹T. Ando, T. Eda, and M. Nakayama, *Solid State Commun.* **23**, 751 (1977).
- ¹²A. Kamgar, *Solid State Commun.* **29**, 719 (1979), and unpublished data on Si(110).
- ¹³B. D. McCombe and T. Cole, *Surf. Sci.* **98**, 469 (1980).
- ¹⁴T. Cole and B. D. McCombe, *J. Phys. Soc. Jpn. Suppl. A* **49**, 959 (1980).
- ¹⁵K. Wiesinger, H. Reisinger, and F. Koch, *Surf. Sci.* **113**, 102 (1982).
- ¹⁶K. S. Yi and J. J. Quinn, *Phys. Rev. B* **27**, 2396 (1983).
- ¹⁷T. Cole, *Surf. Sci.* **113**, 41 (1982).
- ¹⁸W. Beinvogl and F. Koch, *Solid State Commun.* **24**, 687 (1977).
- ¹⁹W. Zawadzki, *J. Phys. C* **16**, 229 (1983).
- ²⁰Y. Takada, K. Arai, N. Uchimura, and Y. Uemura, *J. Phys. Soc. Jpn.* **49**, 1851 (1980).
- ²¹J. Scholz, F. Koch, H. Maier, and J. Ziegler, *Solid State Commun.* **45**, 39 (1982).
- ²²See, for example, A. Pinczuk and J. M. Worlock, *Surf. Sci.* **113**, 69 (1982).
- ²³H. R. Chang and F. Koch, *Surf. Sci.* **113**, 144 (1982).
- ²⁴A. Gold, C. Mazuré, and F. Koch, *Solid State Commun.* (to be published); C. Mazuré, Doctoral dissertation research.
- ²⁵S. Das Sarma, R. K. Kalia, M. Nakayama, and J. J. Quinn, *Phys. Rev. B* **23**, 6832 (1981); **26**, 960 (1982).
- ²⁶F. Schäffler and F. Koch, *Solid State Commun.* **37**, 365 (1981).
- ²⁷S. Das Sarma and B. Vinter, *Phys. Rev. B* **28**, 3639 (1983), and (to be published).
- ²⁸P. Kneschaurek, A. Kamgar, and F. Koch, *Phys. Rev. B* **14**, 1610 (1976).